Field and Petrographic Investigations of the Maw Zone REE Deposit, Athabasca Basin, Saskatchewan

Morteza Rabiei [1], Guoxiang Chi [1] and Charles Normand [2]

Rabiei, M., Chi, G. and Normand, C. (2015): Field and petrographic investigations of the Maw Zone REE deposit, Athabasca Basin, Saskatchewan; *in* Summary of Investigations 2015, Volume 2, Saskatchewan Geological Survey, Saskatchewan Ministry of the Economy, Miscellaneous Report 2015-4.2, Paper A-7, 16p.

Abstract

The Maw Zone rare earth element (REE) deposit, hosted by brecciated pinkish sandstones of the Manitou Falls Formation, represents one of the largest heavy REE and yttrium (Y) concentrations inside the Athabasca Basin in northern Saskatchewan. Hand-held radiospectrometric data indicate equivalent uranium (eU) and equivalent thorium (eTh) concentrations that vary between 0.2 and 7.2 ppm, and between 1.9 and 6.0 ppm, respectively. Where the rocks are more brecciated and altered, sharp increases in eU concentrations and in calculated eU/eTh ratios were detected. Petrographic examination of 86 samples collected from outcrops and drill core shows that the sandstones that host mineralization were subjected to silicification and tourmaline alteration, and contain abundant fractures filled with tourmaline and drusy quartz. Based on paragenetic association and textural relationships, tourmaline can be divided into three generations. Generation "a" formed first, in association with syntaxial quartz. Generation "b", which represents the principal and most pervasively developed stage of tourmaline formation, followed generation "a" and grew within drusy quartz as well as between detrital grains and brecciated rock fragments. The least abundant generation of tourmaline, "c", occurs within drusy quartz in the central part of the veins.

The main ore mineral in this deposit, xenotime, is generally scarce in the samples examined, but is locally abundant and massive. Over an interval of 20 cm in drillhole ZQ-08, at a depth of 75 m, xenotime is concentrated in a few large (several centimetres in diameter) brown patches in the sandstones. Tourmaline is rare in the central part of the mineralized patches, but common near the margins, where it appears to be contemporaneous with xenotime. Textural relationships suggest that the tourmaline accompanying xenotime formed near the beginning of the stage during which generation "b" tourmaline formed. Based on paragenetic relationships established in this study and on tourmaline compositional data, there are clear similarities between the alteration present in the Maw Zone REE deposit and that at the McArthur River uranium deposit. At both locations the main species of tourmaline is magnesiofoitite. Additionally, the tourmaline, which is contemporaneous with the primary stage of uranium mineralization in the McArthur River deposit, occupies the same paragenetic position as, and is texturally identical to, the syn-mineralization tourmaline "b" in the Maw Zone REE deposit.

Keywords: *Maw Zone REE deposit, petrography, tourmaline, xenotime, McArthur River, unconformity-related uranium deposits, paragenesis*

1. Introduction

Anomalous concentrations of light and heavy rare earth elements (REE) have been identified at more than 100 locations in the Athabasca Basin, which is well known for hosting numerous world-class uranium deposits (Normand, 2014). These REE occurrences are locally associated with anomalous concentrations of detrital monazite and zircon, and also hydrothermal uranium oxides, aluminum-phosphate-sulphate minerals (APS), apatite and xenotime (Normand, 2014). The Maw Zone REE deposit, which contains a pre-NI 43-101–compliant resource estimated at 462 664 tonnes averaging 0.21% Y_2O_3, mainly occurring as xenotime, represents one of the largest heavy rare earth

[1] University of Regina, Department of Geology, 3737 Wascana Parkway, Regina, SK S4S 0A2
[2] Saskatchewan Ministry of the Economy, Saskatchewan Geological Survey, 1000-2103 11th Avenue, Regina, SK S4P 3Z8

element (HREE) and Y concentrations inside the Athabasca Basin (Normand, 2014). This deposit is located in the southeastern corner of the basin, between the Key Lake and McArthur River unconformity-related uranium deposits, approximately 5.5 km to the southwest of the relatively newly discovered high-grade Phoenix uranium deposit (Figure 1).

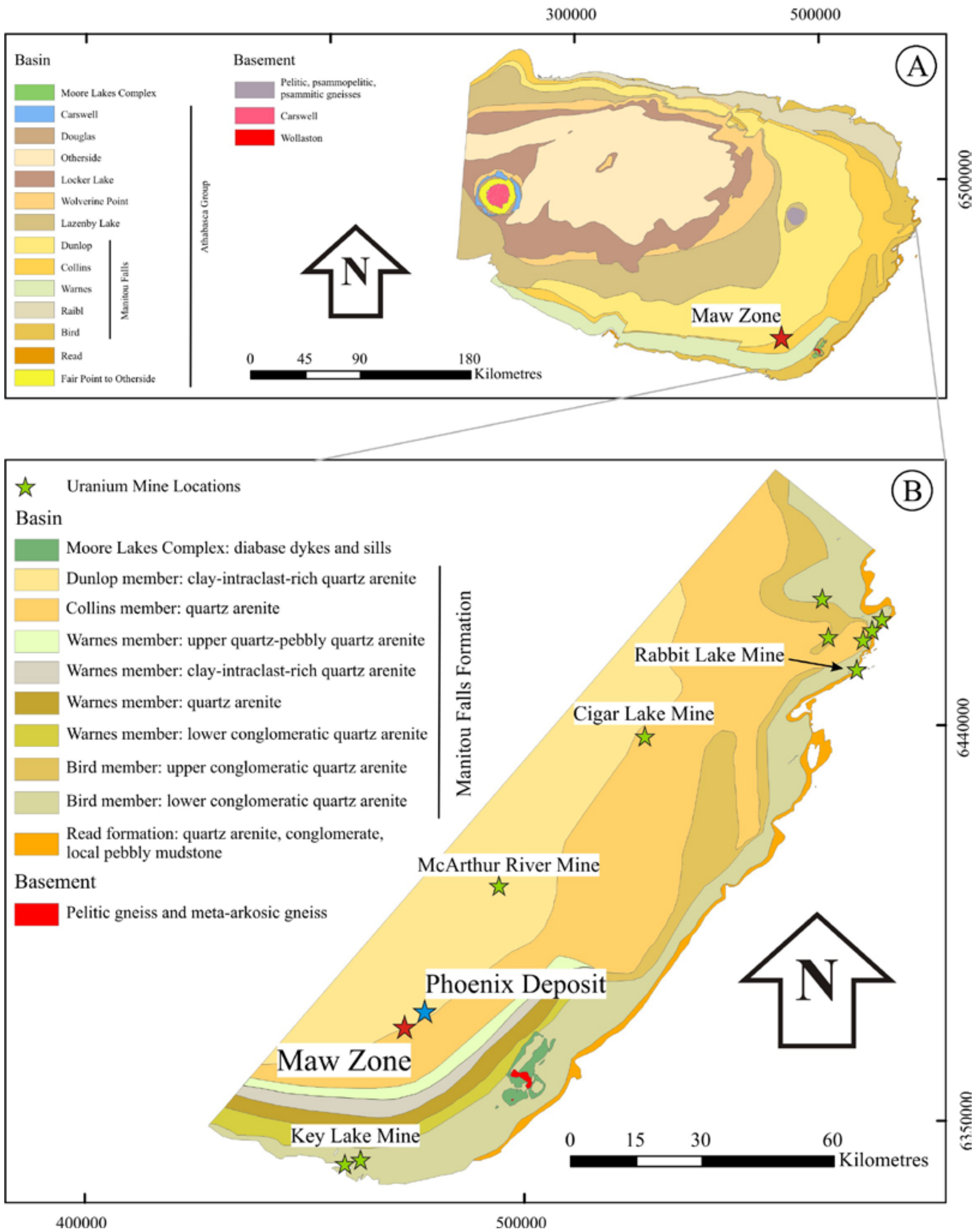

Figure 1 – A) Location map of the Maw Zone REE deposit within the Athabasca Basin, northern Saskatchewan. The bedrock geology is from the 1:250 000-scale map provided in the Saskatchewan Ministry of the Economy's Geological Atlas of Saskatchewan *(http://www.infomaps.gov.sk.ca/website/SIR_Geological_Atlas/SK_Unrestricted_Click_Through_License.htm). B) Map showing lithostratigraphy and location of the Maw Zone REE deposit relative to the unconformity-related uranium mineralization in the southeastern Athabasca Basin. Note the close spatial association and alignment of the Maw Zone with the trend of world-class unconformity-related uranium deposits. The map grid coordinates are given in the UTM system, North American Datum 1983 (NAD83), zone 13N.*

The spatial association of the Maw Zone with unconformity-related uranium deposits led previous geologists to propose that the REE and uranium mineralization precipitated from fluids of similar composition (Quirt *et al*., 1991; Hanly, 2001). However, in a study of radiation-induced defects in quartz, Pan *et al.* (2013) suggested that the fluids responsible for the Maw Zone REE mineralization were low in uranium, and therefore not the same as those responsible for uranium mineralization. Insufficient evidence has been presented to date to support or refute either of these hypotheses. Other investigations published on the mineralogy and geochemistry of adjacent uranium deposits such as McArthur River (*e.g.*, Alexandre *et al*., 2005; Derome *et al*., 2005) have provided insights on the potential genetic relationships between the Maw Zone REE deposit and unconformity-related uranium mineralization. In this paper, we report new petrographic observations and compare them with those reported from nearby uranium deposits, with an emphasis on their similarities in paragenetic sequences. This work will provide the basis for further studies pertaining to the timing of uranium and REE mineralization in the Athabasca Basin.

2. Geological Setting, and Field and Core Observations

a) Geological Setting

The Maw Zone REE deposit was discovered in 1982 during a drilling and mapping program by AGIP Canada Ltd., and was explored thereafter by Union Oil Company of Canada Ltd. Outcrop mapping and geological reports were presented by AGIP Canada Ltd. in 1985 (Saskatchewan Ministry of the Economy (ECON) assessment file 74H06-NW-0080) and later by MacDougall (1990). Structures and alteration exposed at the surface have been mapped by Barker (2007).

Mineralization in the Maw Zone REE deposit is hosted by the Manitou Falls Formation (Figure 1A). This formation is composed mainly of arenite, and is divided into five members including, from bottom to top, Bird, Raibl, Warnes, Collins, and Dunlop. The Maw Zone is located in the Dunlop member (Figure 1B), which is composed of quartz arenite with more than 1% clay intraclasts (Ramaekers *et al*., 2007). The deposit is located above a basement topographic high (based on basement topography from AGIP Canada Ltd. in 1985, ECON assessment file 74H06-NW-0080) partly defined by a northeast-trending quartzite ridge (based on basement geology map by CAMECO Corporation in 2002, ECON assessment file 74H06-NW-0114). This “quartzite” ridge, traditionally believed to represent a metasedimentary unit, has been recently reinterpreted as originating from relatively late-stage magmatic or hydrothermal events that took place in the basement prior to deposition of Athabasca Group sediments, followed by transformation into ridges by pop-up structures relating to outwardly diverging faults (Card, 2012). The Maw Zone is located along one of the faults connected to this pop-up structure.

b) Field Observations

In the Maw Zone, more than 15 outcrops were examined in a 200 x 200 m^2 area, as shown on Figure 2. Nearly all of the outcrops consist of highly silicified, light pinkish to reddish quartz arenite, with locally developed light green alteration (Figures 3A to 3D). The colour of the rock varies according to the intensity and type of alteration present. The earliest and most pervasive type of alteration is silicification, followed by later generations of tourmalinization. A late generation of fracture-filling drusy quartz with associated tourmaline overprints all of the earlier alteration. Hematization is discernible by variations in colour, and overall it is postdated by tourmalinization (Figures 3C to 3F), although multiple generations of hematite are present, as indicated by petrographic study. Moreover, the intensity of the alteration (particularly tourmalinization) is proportional to the intensity of brecciation and fracturing exhibited by the rocks in outcrop (Barker, 2007) and in drill core (Figures 3E, 3F, 4). Brecciation is one of the most important and pervasively developed structural features in the Maw Zone. The breccias are mostly fragment-supported (Figures 3B, 3D, 3F), and are generally characterized by variably sized, subangular fragments (Figure 3). In most cases, the fragments can be pieced together (Figures 3D to 3F), but locally rotated fragments were also observed (Figure 3B). The alteration has locally developed to the point where the rocks have taken on the appearance of clay (Figure 4B), whereas in other cases alteration led to cementation of the fragments, making the host rock appear better lithified (Figure 4A).

The nature of the breccia has been debated by many investigators since the discovery of the mineralized zones. MacDougall (1990) suggested that the brecciation took place soon after deposition, when the sediments were semiconsolidated. In contrast, Quirt *et al.* (1991) interpreted this brecciation as resulting from intense hydrothermal activity, as has been ascribed for breccias in the McArthur River uranium deposit (Kotzer and Kyser, 1990, 1991). Hanly (2001) suggested that brecciation of the sandstones was likely due to desilicification and hydraulic fracturing. Kerr (2010) proposed that the breccias are fault controlled and lie near the intersection of a southeasterly dipping thrust fault and a northeast-dipping normal fault with a downthrow of about 70 m to the north. Barker (2007) suggested that the breccias were generated by faulting, followed by desilicification and then by hydrothermal tourmaline and drusy quartz cementation. Brecciation processes similar to the last model have been proposed for the Shea Creek uranium deposit in the western Athabasca Basin (Lorilleux *et al*., 2001, 2003). Our field and petrographic observations support this last interpretation, *i.e.*, a fault-generated brecciation followed by dissolution of the host sandstone and subsequent tourmalinization and cementation by drusy quartz.

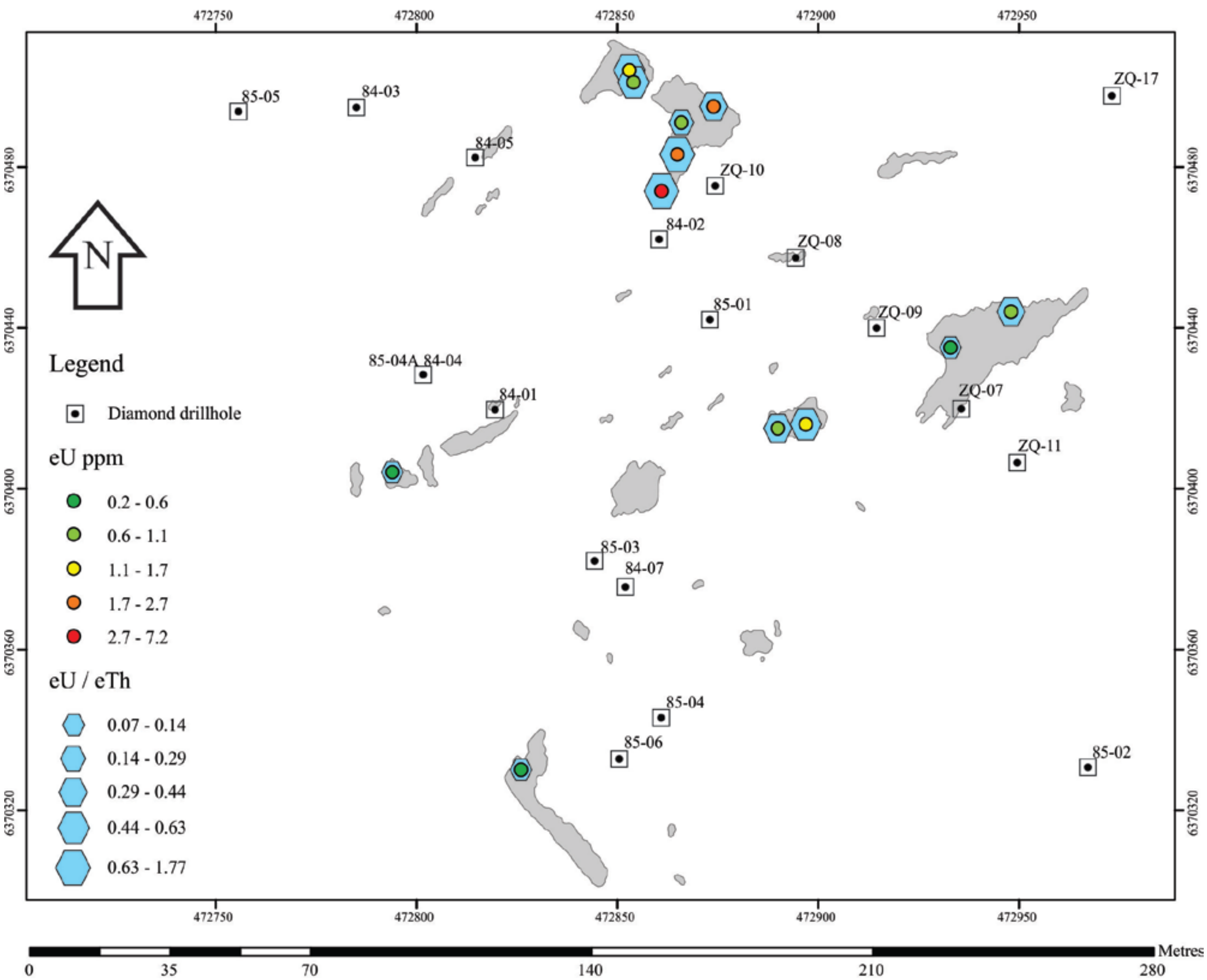

*Figure 2 – Sketch map showing the distribution of outcrops (grey areas) in the Maw Zone REE deposit area (*modified from *MacDougall, 1990) and hand-held radiospectrometer measurements of equivalent uranium (eU) concentrations and equivalent uranium/equivalent thorium (eU/eTh) ratios. Note that both these values increase toward the northern portion of the map area, where brecciation and alteration are most intensely developed. The grid coordinate system is the same as in Figure 1. Locations of diamond drillholes are from ECON assessment files 74H06-NW-0080 and 74H-06-NW-0114.*

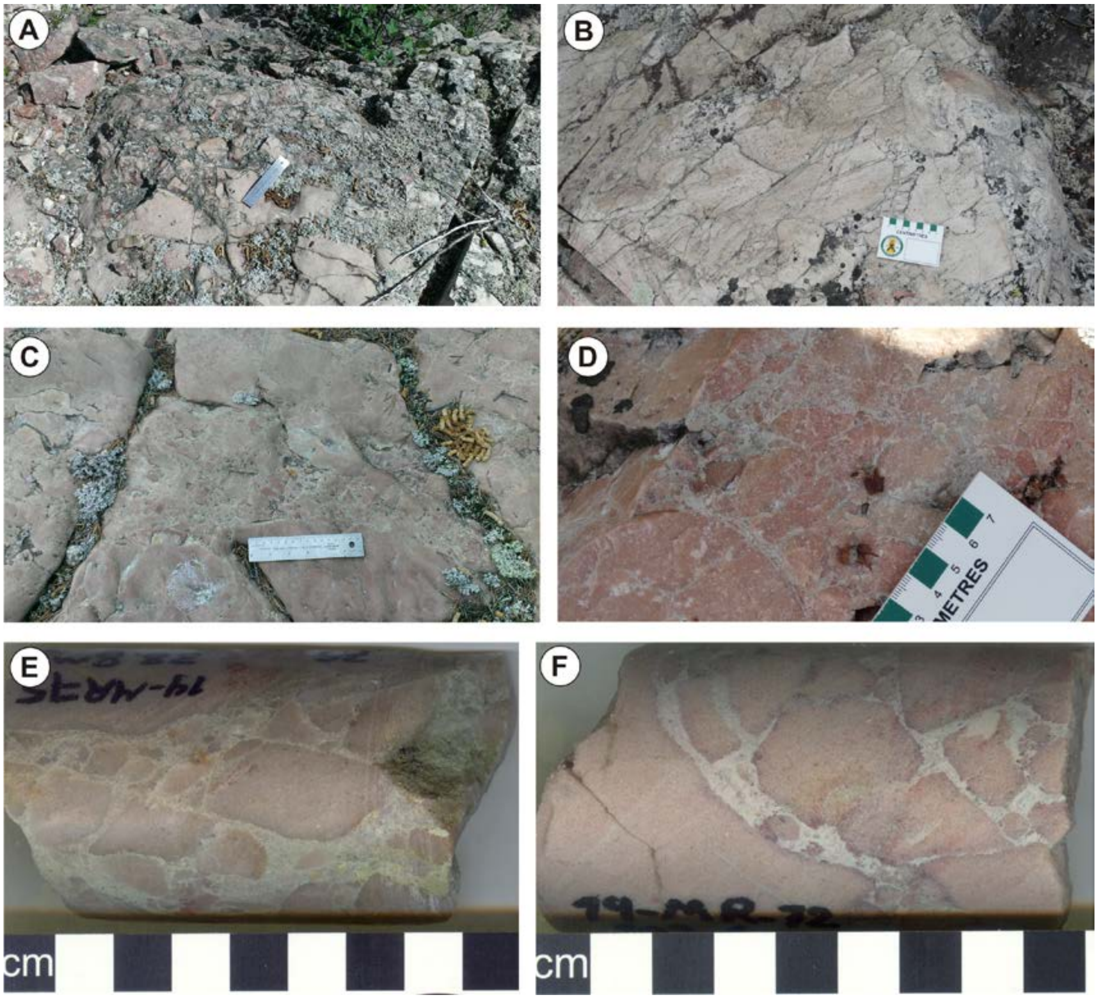

Figure 3 – Photographs showing macroscopic features of brecciated sandstones in outcrop (A to D) and drill core (E and F) from the Maw Zone deposit: A) wide variation in size of the fragments; B) fragment-supported and mosaic textures; C) brecciated sandstone with pale green tourmaline cement; D) brecciated hematized sandstone with pale green tourmaline cement; E) and F) show drill core segments composed of sandstone breccias cemented by tourmaline in borehole 85-01 at depths of 38.8 m and 102.6 m, respectively. (Ruler in photos A and C is 15 cm (6 inches) long.)

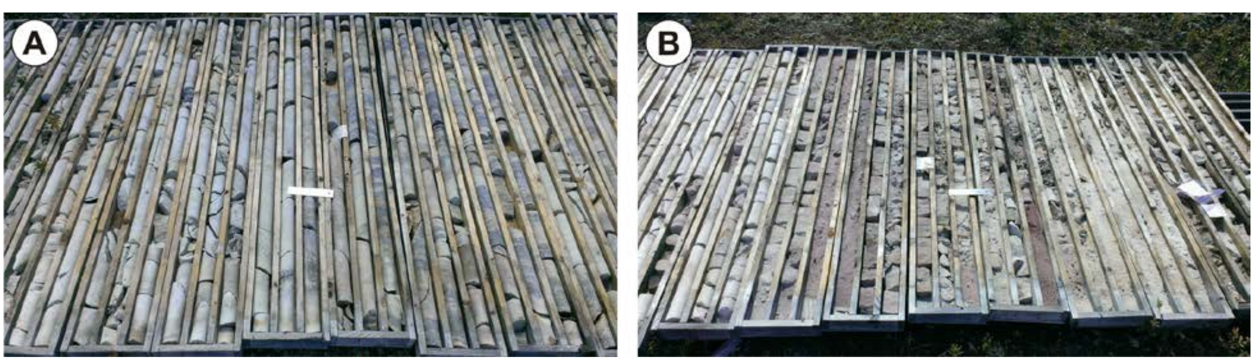

Figure 4 – Photographs showing core from borehole ZQ-09: A) example of brecciated and altered sandstone from depths of approximately 160 to 190 m, where silica alteration has cemented the brecciated fragments so that the rock appears unbrecciated; B) extensively fractured and highly altered sandstone from depths of approximately 30 to 60 m, where the degree of alteration makes the rock appear clay-like. (Note: depth increases from left to right in each photo, and from top to bottom in the core boxes; ruler is 15 cm (6 inches) long.)

c) Hand-held Radiospectrometer Measurements

Equivalent uranium (eU) and equivalent thorium (eTh) concentrations ranging from 0.2 to 7.2 ppm and from 1.9 to 6.0 ppm, respectively, were obtained from measurements in the field using a hand-held gamma-ray spectrometer. The calculated eU/eTh ratios using the above concentrations vary between 0.07 and 1.76. The data show that there is an increase in eU concentrations towards the northern extremity of the studied outcrop area (see Figure 2), where rocks are more brecciated and altered. The increase in magnitude of the calculated eU/eTh values shown on Figure 2 roughly parallels the increase of the measured eU values, suggesting that the presence of a U-bearing and comparatively Th-poor phase caused the spectrometer response. The highest eU/eTh value of 1.77 (Figure 2) was identified in outcrops where elevated HREE+Y concentrations were obtained from bulk sample analyses in the past (ECON assessment file 74H06-NW-0080; MacDougall, 1990). The eU/eTh ratio of 1.77 from this study is comparable to the U/Th ratios of 1.40, 2.01 and 1.15 calculated from electron microprobe data for the Maw Zone presented in Hanly (2001) for his sample 85-5-6, which was collected from breccia containing massive xenotime associated with tourmaline and Fe-oxide.

d) Mineralization Features in Hand Samples

Previous studies have indicated that xenotime [$(HREE,Y)PO_4$] is the most important ore mineral in the Maw Zone deposit (Hanly, 2001). Because there is a great similarity in the appearance of xenotime and iron hydroxide minerals in hand specimen, and owing to the fact that both are very fine grained, finding a hand sample that unequivocally contains xenotime has proven challenging. Nonetheless, guided by chemical analyses from boreholes published by AGIP Canada Ltd. in 1985 (ECON assessment file 74H06-NW-0080), two samples were identified from drillhole ZQ-08 at depths of 75.0 m and 75.2 m, in which xenotime aggregates occur as large, centimetre-sized, brown patches (Figure 5). These mineralized patches are not conformable with the bedding (Figure 5; note the bedding is at a high angle to the sides of the core). In addition to the occurrence as large, patchy aggregates, there are several other modes of occurrence of the xenotime in the Maw Zone deposit, including as disseminations and aggregates in fractures and in the matrix of breccias, as rims coating detrital quartz grains, as pore space fillings, and as rims around, and almost complete replacements of, zircon (Quirt *et al*., 1991; Hanly, 2001). Most of the latter occurrences are not discernable in hand sample and can only be studied in thin section.

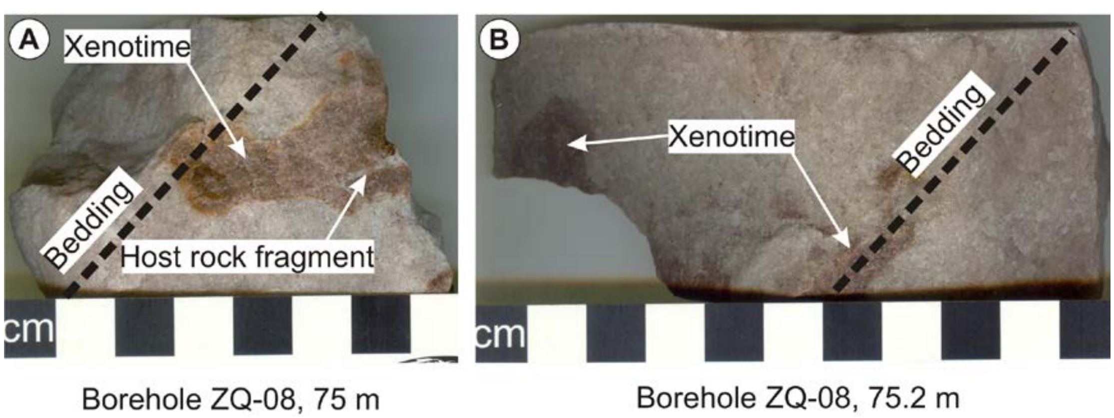

Figure 5 *– Photographs showing drill core samples that carry massive, brown patches of xenotime.*

3. Petrography and Paragenetic Sequence

A total of 86 polished thin sections were examined for petrography. The focus was on quartz, tourmaline, hematite and xenotime, and their relative timing.

a) Quartz

There are three main types of quartz in the Maw Zone area, including detrital quartz, syntaxial quartz and drusy quartz.

Detrital quartz grains are mostly uniform in size and show good roundness and sorting (Figure 6A). Poorly developed graded bedding is rarely observed (Figures 6C, 6D). The size of the detrital grains mostly ranges from 0.1 to 0.5 mm, but grains measuring less than 0.05 mm or more than 1 mm in diameter are also commonly observed (Figures 6B, 6E, 6F). Detrital grains are in point, long, and concave-convex contact with each other in areas of least alteration and mineralization, but may appear to float in the matrix in areas of strong alteration and mineralization (Figures 6E, 6F).

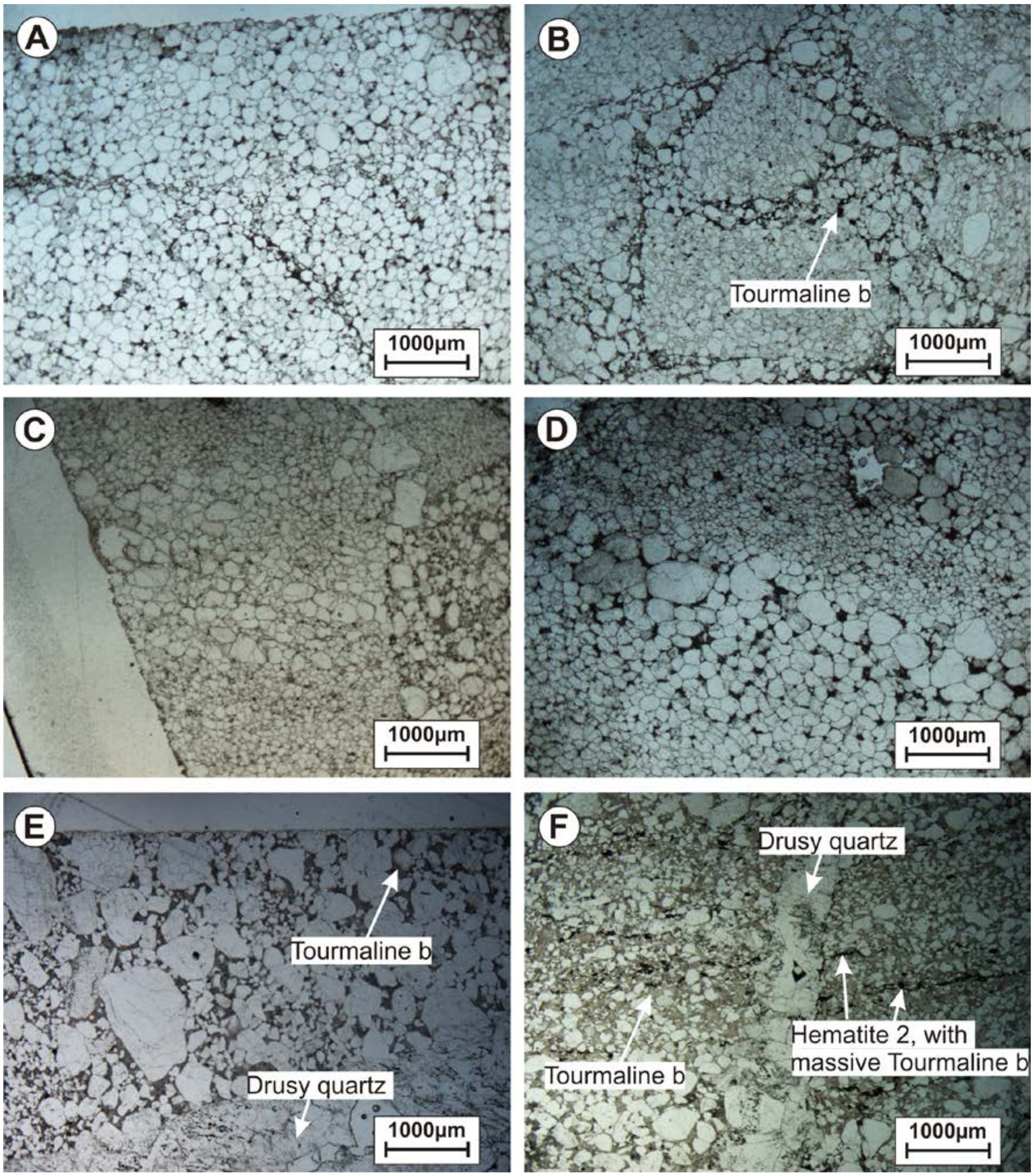

Figure 6 – Polished thin section photomicrographs showing common features exhibited by detrital quartz in the host rocks: A) textural features (grain size and contacts) commonly observed in unaltered sandstone; B) brecciation and the effects of alteration events that subsequently modified the texture and grain contacts in the sandstone; C) and D) graded bedding; E) local poor sorting. F) Photomicrograph of sandstone showing graded bedding and tourmaline alteration exclusively in the matrix. Also shown in this photo are lineated patches of dark hematite coexisting with tourmaline in the matrix, and a vein of drusy quartz cutting across the bedding.

Syntaxial quartz is the second most common form of quartz in the Maw Zone deposit. At least two generations of syntaxial quartz were observed in thin section. The first generation overgrows detrital quartz grains and generally contains iron oxide. This generation of syntaxial quartz appears to predate brecciation (Figures 7A, 7B). The second generation of syntaxial quartz is much more common than the first and is coeval with the first generation of hydrothermal tourmaline (Figures 7C, 7D). Drusy quartz that grew in crystallographic continuity with the second generation of syntaxial quartz forms euhedral quartz crystals that project into open spaces (Figures 7E, 7F).

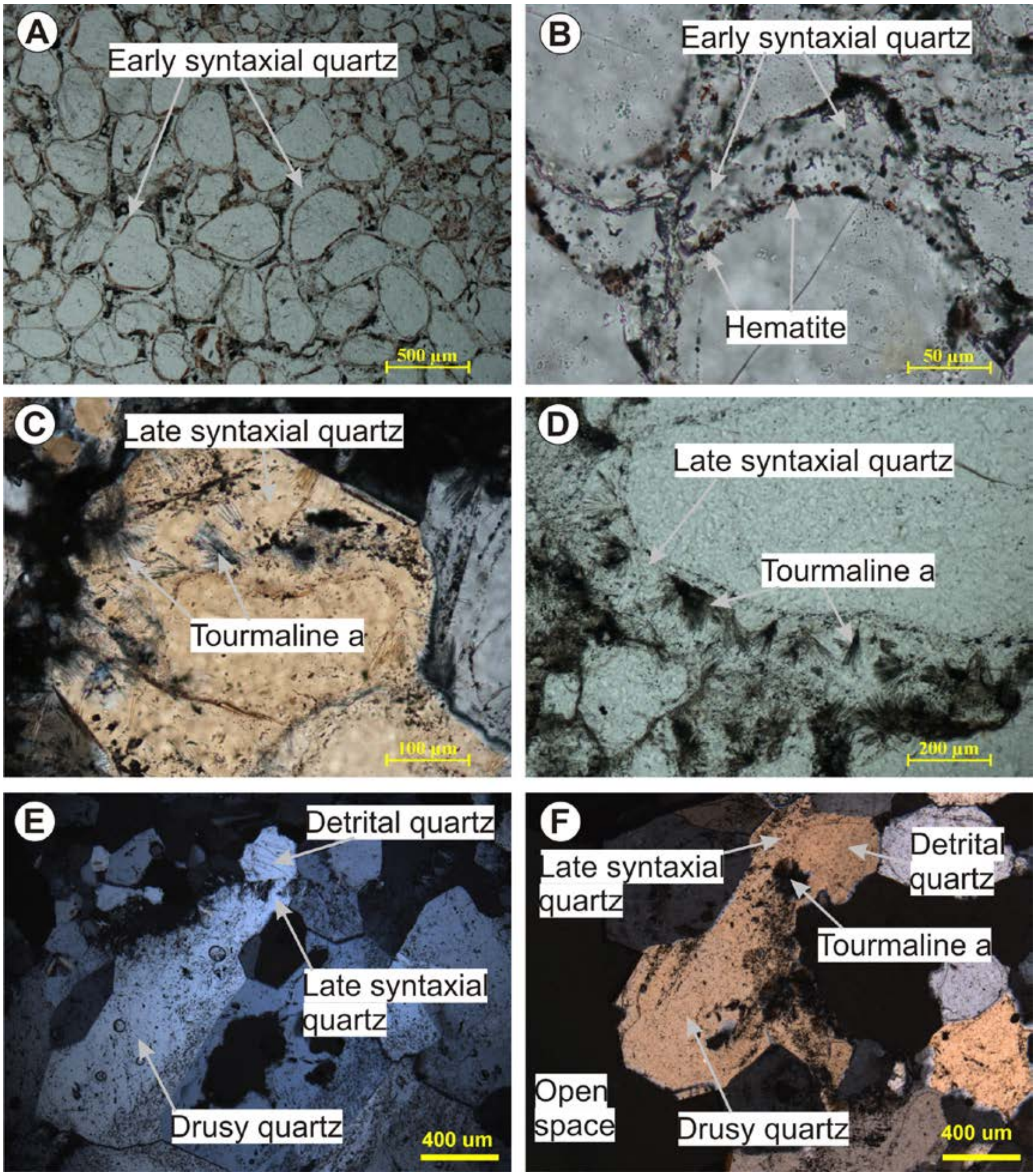

Figure 7 – A series of polished thin section photomicrographs that illustrate different textural relationships exhibited by various generations of syntaxial and drusy quartz: A) and B) show a first generation of syntaxial quartz that predates brecciation, formed without tourmaline and grew over detrital quartz and after flaky hematite (H1); C) and D) show a second generation of syntaxial quartz that is accompanied by the formation of early prismatic tourmaline (tourmaline "a"); E) and F) photomicrographs (crossed polars) display drusy quartz that grew in crystallographic continuity with a second generation of syntaxial quartz. Continuity of growth between syntaxial and drusy quartz is revealed by similar birefringence and extinction in adjacent syntaxial and drusy quartz. Patches of tourmaline "a" formed locally at the transition between late syntaxial quartz and drusy quartz.

The third form of quartz is drusy quartz, which is best developed in veins. The size and distribution of drusy quartz crystals vary widely (Figures 8A, 8B). In some instances, drusy quartz fills open spaces and in others it occurs as a cement in breccia (Figures 8C, 8D). In places, drusy quartz grew in crystallographic continuity with syntaxial quartz, and in others the drusy quartz nucleated directly from the walls of fractures without evidence of topotaxy (Figures 7E, 7F, 8A). Distinction between the different stages of drusy quartz can be made using the different stages of tourmaline that coexist with them (Figures 8E, 8F).

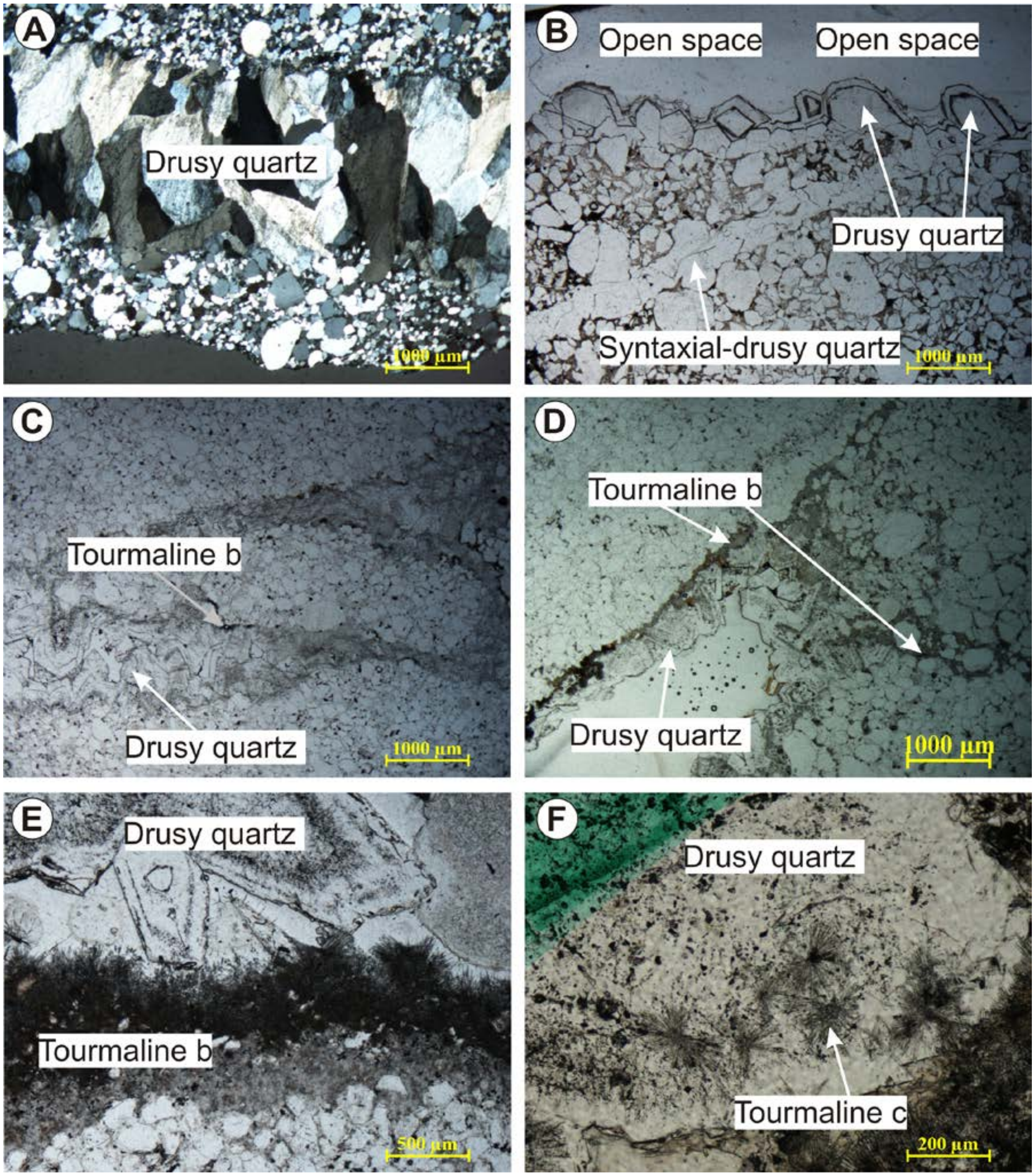

Figure 8 – A series of polished thin section photomicrographs that illustrate different textural relationships exhibited by various generations of drusy quartz: A) vein consisting of euhedral, drusy quartz crystals with their long axes perpendicular to the vein wall; B) well-developed syntaxial quartz along the wall of a fracture, which is connected to a veinlet consisting of drusy quartz; C) and D) drusy quartz together with tourmaline "b" cementing breccia and filling open spaces caused by brecciation; E) tourmaline "b" filling open space associated with drusy quartz; F) latest generation of tourmaline ("c") formed within drusy quartz.

b) Tourmaline

At the macroscopic scale, tourmaline is observed predominantly in veins or as cements in breccias (see Figure 3). Individual crystals of the mineral are very fine grained, however, making the mineral difficult to recognize with the naked eye. Where abundant, tourmaline imparts a whitish green to green colour to hand samples (Figures 3B, 3E, 3F). Hanly (2001) recognized two major types of tourmaline in the Maw Zone area, based on their composition, colour and mode of occurrence. These types comprised alkali-free dravite and alkali-free chromian dravite. According to Hanly (2001), chromium dravite always displays a green colour and occurs within fractures, in the matrices of breccias, and intergrown with euhedral quartz in fractures and vugs. The alkali-free dravite is commonly white but can also be pale green or blue and occurs in a variety of modes: as crystals within quartz overgrowths on detrital quartz; as crystals in pore spaces that are intergrown with, or postdate, syntaxial quartz cement; as aggregates of crystals in fractures and matrices of breccias; as crystals intergrown with, or coating, euhedral quartz-filled fractures and vugs; as aggregates of crystals in stylolitic seams with heavy minerals; and as overgrowths on detrital schorl-dravite (Hanly, 2001).

In order to confirm Hanly's (2001) designation of alkali-free dravite and alkali-free chromian dravite, his electron microprobe tourmaline analyses were plotted using the Tourmaline Mineral Recalculation software of Andy Tindle, of the Open University, Milton Keynes, UK (http://www.open.ac.uk/earth-research/tindle/AGTWebPages/AGTSoft.html) (Figure 9). The results show that all of the tourmaline in the Maw Zone plots as magnesiofoitite rather than dravite. The existence of magnesiofoitite as a tourmaline species in the Maw Zone was also noted by Chen *et al.* (2015).

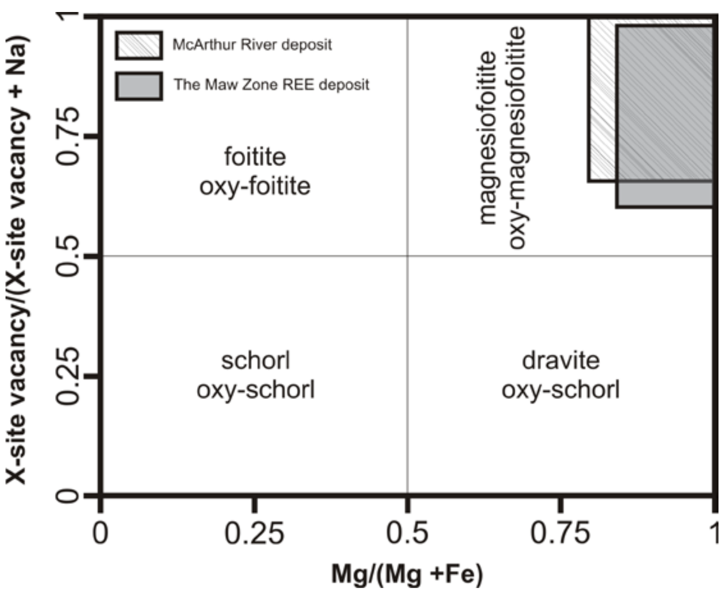

***Figure 9** – Mg/(Mg+Fe)* vs *X-site occupancy (X-site vacancy/(X-site vacancy + Na)) discrimination plot showing the compositional fields of the vacant-subgroup 1 species foitite and magnesiofoitite, of the alkali-subgroups 1 and 2 species schorl and dravite, and the oxy species of the tourmaline supergroup (Henry* et al.*, 2011), as calculated from electron microprobe analyses presented in Hanly (2001). Significant overlap between the compositional fields of tourmaline from the Maw Zone REE deposit and the McArthur River uranium deposit suggests that they formed from fluids that shared comparable physicochemical characteristics.*

Our analysis demonstrated that all tourmaline from the Maw Zone can be grouped into three different types, "a", "b" and "c", based on their paragenetic position, crystal habit and mineral associations. However, we cannot define specific gaps in time between each episode of tourmaline mineralization because in many cases the tourmaline mineralization took place continuously from the earlier to the later stages without any recognizable discontinuity.

The earliest episode of tourmaline formation, "a", includes tourmaline that co-precipitated with early syntaxial quartz (Figures 7C, 7D). Tourmaline "b" formed in a much wider range of occurrences, including aggregates between detrital quartz grains (Figures 10A to 10D), cementing breccia (Figures 3E, 3F, 8D, 10B, 10E, 10F), and filling open spaces (Figures 8C, 8E). Large amounts of tourmaline "b" precipitated during the dissolution of the host sandstone that accompanied breccia development (Figures 10A, 10B). The latest phase of tourmaline ("c") has limited distribution. In most instances, there is clear evidence that this tourmaline formed together with drusy quartz (Figure 8F).

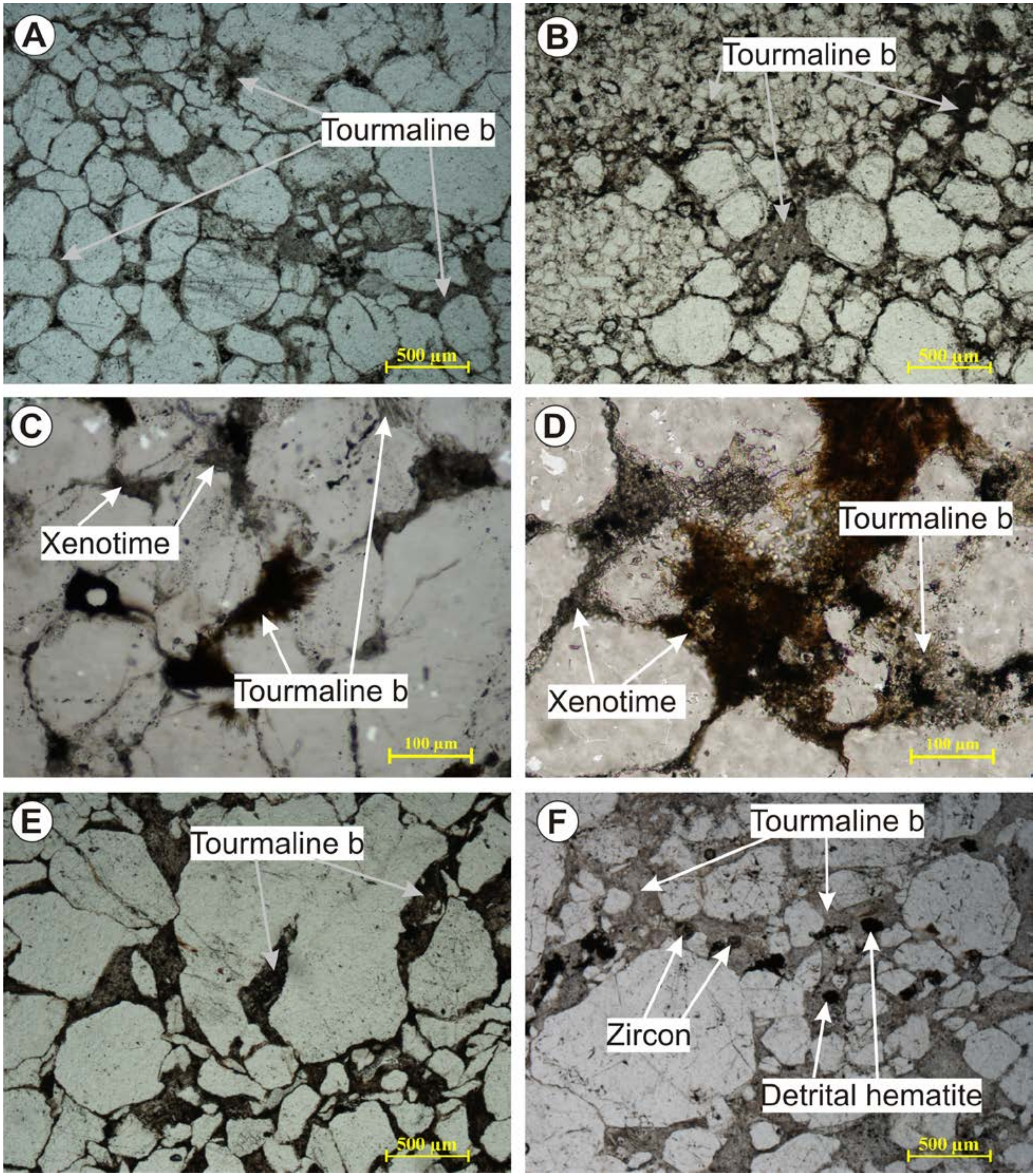

Figure 10 – A series of polished thin section photomicrographs showing various modes of occurrence of tourmaline "b" in the Maw Zone REE deposit: A) and B) show tourmaline "b" occurring between detrital quartz grains and as a cement of breccias; C) and D) show tourmaline and xenotime coexisting between detrital quartz grains; E) and F) show tourmaline "b" as a cement of breccias.

c) Hematite

The widespread development of hematite and/or iron hydroxides can be recognized in outcrop and drillhole samples by colour variations from red to purple and brown. Our petrographic studies indicate several phases of hematite in the paragenetic sequence. The earliest phase is rounded detrital hematite (Figure 11A). The next generation (H1) is represented by flakes of hematite developed on the rims of detrital quartz (Figures 7B, 11B, 11C) and is spatially associated with the early phase of syntaxial quartz. The most pervasive phase of hematization is coeval with the formation of tourmaline "b". This phase (H2), like the contemporaneous tourmaline, occurs between brecciated sandstone fragments (Figure 11D) and detrital quartz grains (Figure 11E). The latest phase of hematite (H3) partially fills open, and overprints previously formed, fractures (Figure 11F).

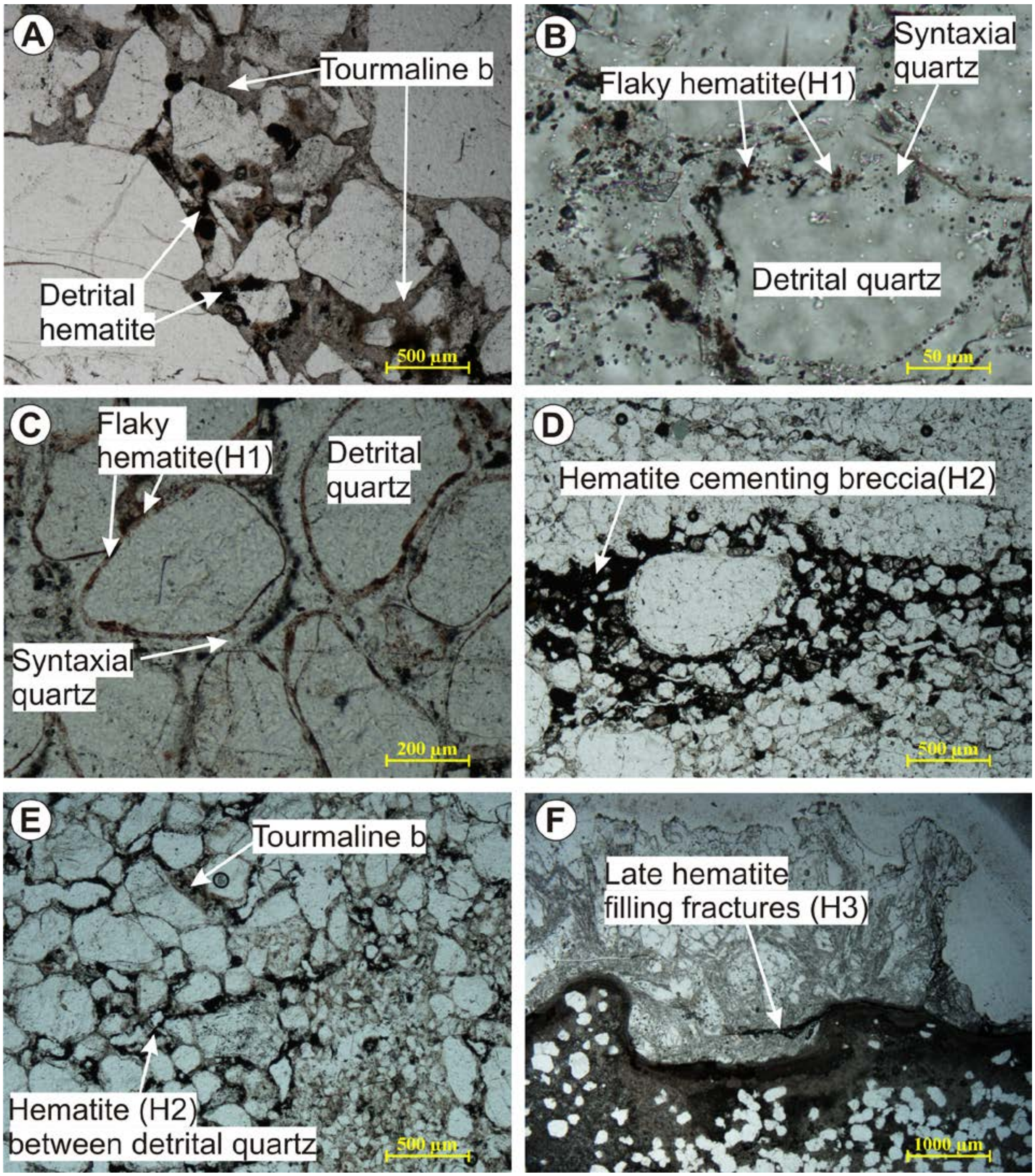

Figure 11 – A series of photomicrographs showing different modes of occurrence of hematite: A) detrital hematite cemented by tourmaline "b"; B) and C) flaky hematite (H1) forming partial rims around detrital quartz grains; D) massive hematite (H2) cementing breccia; E) hematite (H2) coexisting with tourmaline "b" between detrital grains; F) latest generation of hematite (H3) filling open spaces and fractures.

d) Xenotime

Xenotime in the Maw Zone REE deposit area is the most important mineral carrying HREEs and Y. Another mineral phase reported to carry HREEs and Y is bastnaesite, which occurs along fractures and around detrital zircon grains in the Maw Zone (Chen *et al*., 2015).

Xenotime was only rarely observed in samples collected from the mineralized zone. As mentioned above in section 2d, however, local concentrations were noted, occurring as irregular centimetre-sized brown patches in silicified sandstone (see Figure 5). Micron-scale xenotime crystals occur between detrital quartz grains and replace the latter (Figures 12A to 12D). The xenotime crystals are coeval with tourmaline "b" (Figures 12E, 12F).

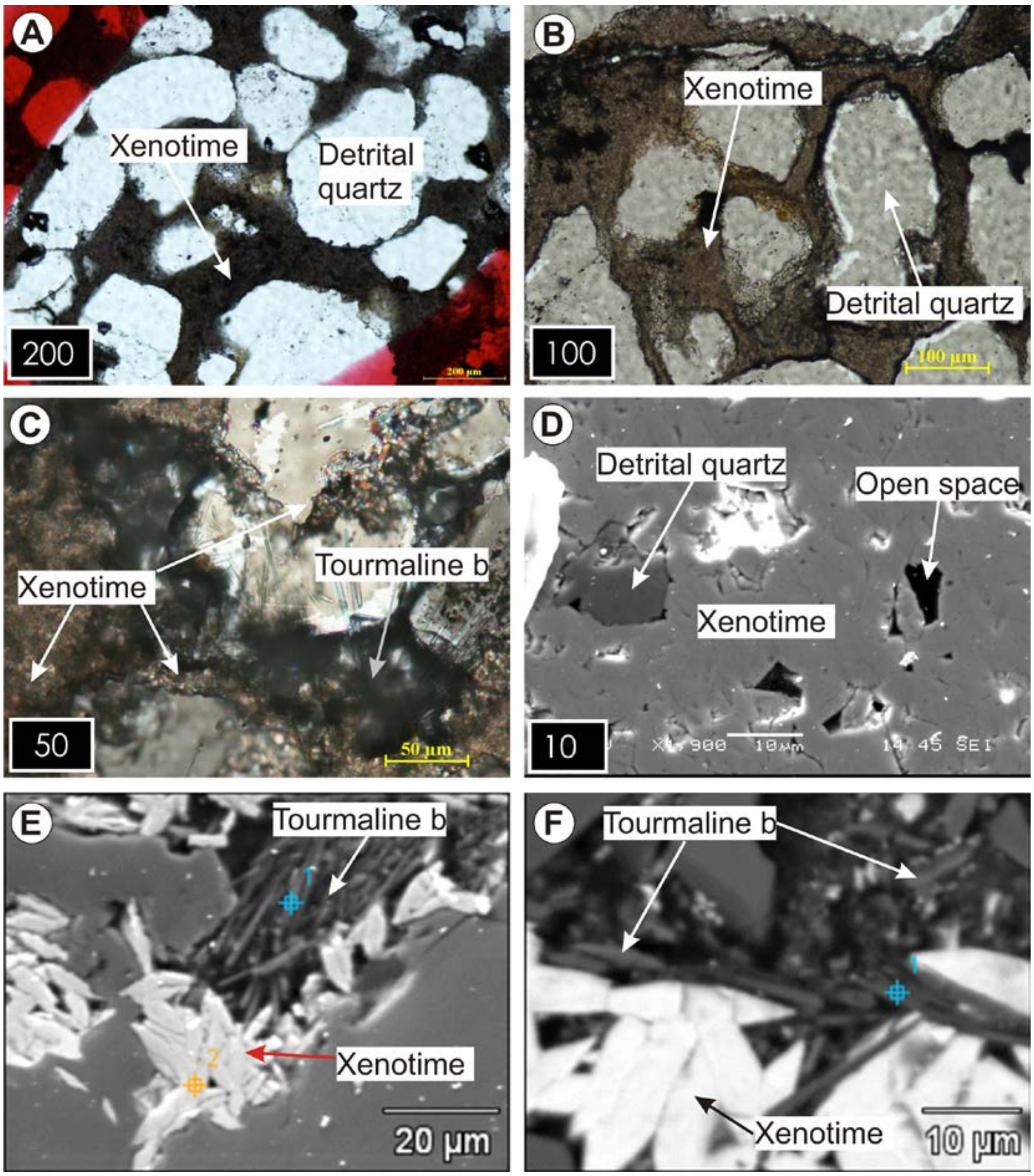

Figure 12 – A series of photomicrographs and scanning electron microscope (SEM) images showing the different styles of xenotime mineralization in the Maw Zone REE deposit: A) and B) show massive, fine-grained xenotime occurring as a replacement of detrital quartz grains; C) illustrates the close paragenetic relationship between xenotime and tourmaline "b". D) SEM image showing detail of a massive aggregate of fine-grained, anhedral xenotime crystals. E) and F) Close-up SEM views of coexisting xenotime and tourmaline crystals; mutually sharp contacts between the two intergrown minerals suggest co-precipitation.

In the photomicrographs shown in Figures 12A and 12B, the detrital quartz grains appear to ‘float’ in a matrix of xenotime, which might be taken to suggest that mineralization took place during early diagenesis (before significant compaction). However, careful examination of areas inside and outside the mineralized areas in thin section and SEM images reveals that the number of detrital grains per viewed area are similar, indicating instead that mineralization took place by replacement after compaction.

e) Paragenetic Sequence

The paragenetic sequence established in this study for the Maw Zone REE deposit is shown in Figure 13. Early detrital components include quartz, zircon, muscovite and hematite. Hematite is also present as a product of early diagenesis, rimming detrital quartz grains and predating the early phases of diagenetic quartz overgrowth (Figure 7B).

No tourmaline accompanied precipitation of early diagenetic syntaxial quartz. This early syntaxial quartz was followed by the precipitation of a second generation of syntaxial quartz that formed contemporaneously with an early generation of tourmaline (tourmaline “a”). This stage is considered to correspond to the initiation of tourmaline alteration. In a continuous process, tourmaline “b” followed the earlier generation of tourmaline and was precipitated in drusy quartz; it also occurs extensively as cement in the brecciated host sandstone. The main phase of xenotime precipitation occurred during this time, contemporaneous with tourmaline “b” and the beginning of drusy quartz precipitation. The later mineral phases include drusy quartz together with less abundant tourmaline “c” and thin hematite veins.

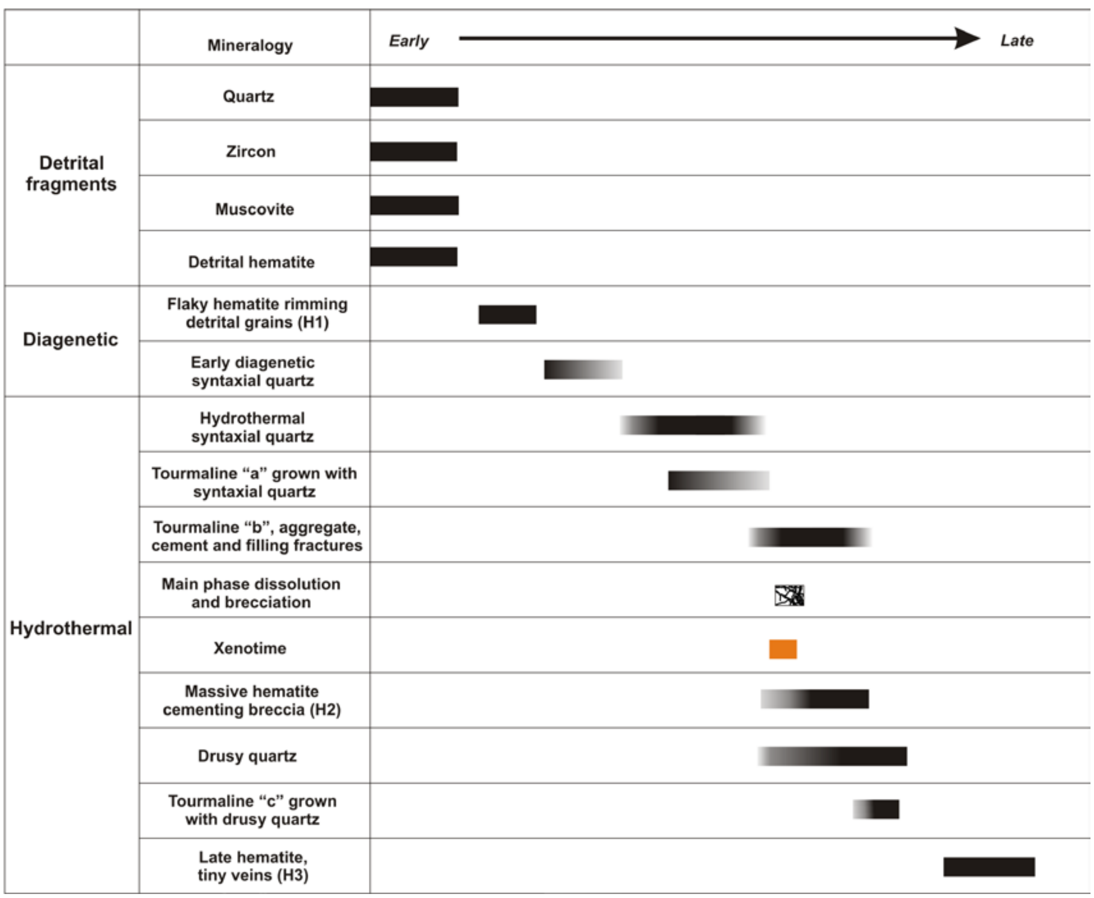

Figure 13 – Diagram illustrating the paragenetic sequence of events and mineral formation in the Maw Zone REE deposit. The gradations in fill of some of the boxes indicate a gradual phasing in and/or phasing out of that mineral growth.

The results of our petrographic studies on the Maw Zone REE deposit, combined with previous studies published on the McArthur River uranium deposit (*e.g.*, Derome *et al*., 2005), show that significant similarities exist between the two. Specifically, the episodic "b" tourmaline in the Maw Zone occupies the same paragenetic position as the syn-mineralization "dravite 2" in the McArthur River uranium deposit, and both of them have the magnesiofoitite composition (Figure 9). Therefore, it is inferred that the REE mineralization in the Maw Zone deposit, which has been shown to be coeval with stage "b" tourmaline, was formed at the same time as uranium mineralization in the nearby unconformity-related uranium deposits.

4. Conclusions

The following conclusions are drawn from our field and petrographic studies of the Maw Zone REE deposit:

1) The REE mineralization is related to brecciation and tourmaline alteration. The brecciation was likely initiated by fault-related fracturing and enhanced by dissolution of hosting sandstone, followed by tourmaline alteration, silicification and xenotime precipitation.

2) Although uranium concentrations are low in the mineralized zones, equivalent uranium (eU) and equivalent thorium (eTh) concentrations measured with a hand-held radiospectrometer, as well as calculated eU/eTh concentration ratios, appear to be highest where the brecciation is most intense and the REE mineralization occurs. Calculated eU/eTh ratios from this study are consistent with the U/Th ratios reported by Hanly (2001) for electron microprobe analysis of xenotime from the Maw Zone REE mineralization.

3) Most of the REE mineralization cannot be visibly identified in the field or in drill core; however, brown, centimetre-sized patches enriched in xenotime can be locally found.

4) The tourmaline in the Maw Zone deposit can be divided into three stages, "a", "b" and "c", of which the second stage ("b") is contemporaneous with xenotime. The stage "b" tourmaline in the Maw Zone occupies the same paragenetic position as the syn-mineralization tourmaline ("dravite 2" of Derome *et al.*, 2005) in the McArthur River uranium deposit, suggesting that the REE mineralization and uranium mineralization in the area have similar timing.

5. Acknowledgments

This paper reports on results of the first year of a multi-year study. This study is mainly supported by the Saskatchewan Ministry of the Economy and a Natural Sciences and Engineering Research Council (NSERC) Discovery grant to Normand and in part by an NSERC Discovery grant to Chi. Zenghua Li and Kewen Wang are thanked for their assistance in the fieldwork, and Ken Ashton is thanked for help in core observation, discussion, and review of this paper. We are grateful to Denison Mines for accommodation during our fieldwork.

6. References

Alexandre, P., Kyser, K., Polito, P. and Thomas, D. (2005): Alteration mineralogy and stable isotope geochemistry of Paleoproterozoic basement-hosted unconformity-type uranium deposits in the Athabasca Basin, Canada; Economic Geology, v.100, p.1547-1563.

Barker, M. (2007): Structural analysis of the Maw zone: a sub-economic REE deposit; B.Sc. thesis, St.Francis Xavier University, Antigonish, Nova Scotia, 82p.

Card, C.D. (2012): The origins of anomalously graphitic rocks and quartzite ridges in the basement to the southeastern Athabasca Basin; *in* Summary of Investigations 2012, Volume 2, Saskatchewan Geological Survey, Saskatchewan Ministry of the Economy, Miscellaneous Report 2012-4.2, Paper A-6, 15p.

Chen, S., Hattori, K., Grunsky, E.C. and Liu, Y. (2015): Principal component analysis and REE-hosting minerals of sandstones in the REE-rich Maw Zone, Athabasca Basin, Saskatchewan; Geological Survey of Canada, Scientific Presentation 32, poster. doi: 10.4095/296514.

Derome, D., Cathelineau, M., Cuney, M., Fabre, C., Lhomme, T. and Banks, D.A. (2005): Mixing of sodic and calcic brines and uranium deposition at McArthur River, Saskatchewan, Canada: a Raman and laser-induced breakdown spectroscopic study of fluid inclusions; Economic Geology, v.100, p.1529-1545.

Hanly, A.J. (2001): The mineralogy, petrology and rare earth element geochemistry of the Maw zone, Athabasca Basin, Canada; M.Sc. thesis, University of Missouri, Rolla, Missouri, 168p.

Henry, D.J., Novak, M., Hawthorne, F.C., Ertl, A., Dutrow, B.L., Uher, P. and Pezzotta, F. (2011): Nomenclature of the tourmaline-supergroup minerals; Amercian Mineralogist, v.96, p.895-913.

Kerr, W. (2010): The discovery of the Phoenix deposit: a new high-grade, Athabasca Basin unconformity-type uranium deposit, Saskatchewan, Canada; *in* The Challenge of Finding New Mineral Resources: Global Metallogeny, Innovative Exploration, and New Discoveries, Volume 2: Zinc-Lead, Nickel-Copper-PGE, and Uranium, Goldfarb, R.J., Marsh, E.E. and Monecke, T. (eds.), Society of Economic Geologists, Special Publication No.15, p.703-728.

Kotzer, T.G. and Kyser, T.K. (1990): The use of stable and radiogenic isotopes in the identification of fluids and processes associated with unconformity-type uranium deposits; *in* Modern Exploration Techniques, Beck, L.S. and Harper, C.T. (eds.), Saskatchewan Geology Society, Special Publication 10, p.115-131.

Kotzer, T.G. and Kyser, T.K. (1991): Retrograde alteration of clay minerals in uranium deposits: Radiation catalyzed or simply low temperature exchange?; Chemical Geology (Isotope Geoscience Section), v.86, p.307-321.

Lorilleux, G., Cuney, M., Jébrak, M., Rippert, J.C. and Portella, P. (2003): Chemical brecciation processes in the Sue unconformity-type uranium deposits, eastern Athabasca Basin (Canada); Journal of Geochemical Exploration, v.80, p.241-258.

Lorilleux, G., Jébrak, M., Cuney, M. and Baudemont, D. (2001): Polyphased hydrothermal breccias associated with unconformity type uranium mineralization (Canada): from fractal analysis to structural significance; Journal of Structural Geology, v.24, p.323-338.

MacDougall, D.G. (1990): Rare earth element mineralization in the Athabasca Group – Maw zone; *in* Summary of Investigations 1990, Saskatchewan Geological Survey, Saskatchewan Energy and Mines, Miscellaneous Report 90-4, p.103-105.

Normand, C. (2014): Rare Earths in Saskatchewan: Mineralization Types, Settings, and Distributions; Saskatchewan Ministry of the Economy, Saskatchewan Geological Survey, Report 264, 105p.

Pan, Y., Yeo, G., Rogers, B., Austman, C. and Hu, B. (2013): Application of radiation-induced defects in quartz to exploration for uranium deposits: a case study of the Maw Zone, Athabasca basin, Saskatchewan; Exploration and Mining Geology, v.21, p.115-128.

Quirt, D.H., Kotzer, T. and Kyser, T.K. (1991): Tourmaline, phosphate minerals, zircon and pitchblende in the Athabasca Group: Maw zone and McArthur River areas, Saskatchewan; *in* Summary of Investigations 1991, Saskatchewan Geological Survey, Saskatchewan Energy and Mines, Miscellaneous Report 91-4, p.181-191.

Ramaekers, P., Jefferson, C.W., Yeo, G.M., Collier, B., Long, D.G., Catuneanu, O., Bernier, S., Kupsch, B., Post, R., Drever, G., McHardy, S., Jiricka, D., Cutts, C. and Wheatley, K. (2007): Revised geological map and stratigraphy of the Athabasca Group, Saskatchewan and Alberta; *in* EXTECH IV: Geology and EXploration TECHnology of the Proterozoic Athabasca Basin, Saskatchewan and Alberta, Jefferson, C.W. and Delaney, G. (eds.), Geological Survey of Canada Bulletin 588 / Saskatchewan Geological Society Special Publication 18 / Geological Association of Canada, Mineral Deposits Division, Special Publication 4, p.155-191.